

PAPER • OPEN ACCESS

The bioclimatic extent and pattern of the cold edge of the boreal forest: the circumpolar taiga-tundra ecotone

To cite this article: Paul M Montesano *et al* 2020 *Environ. Res. Lett.* **15** 105019

View the [article online](#) for updates and enhancements.

You may also like

- [Lipophilic Additives for Highly Concentrated Electrolytes in Lithium-Sulfur Batteries](#)
Ka-Cheong Lau, Nancy L. Dietz Rago and Chen Liao
- [FIRST-YEAR RESULTS OF BROADBAND SPECTROSCOPY OF THE BRIGHTEST FERMI-GBM GAMMA-RAY BURSTS](#)
Elisabetta Bissaldi, Andreas von Kienlin, Chryssa Kouveliotou et al.
- [Fluorinated Electrolytes for Li-S Battery: Suppressing the Self-Discharge with an Electrolyte Containing Fluoroether Solvent](#)
Nasim Azimi, Zheng Xue, Nancy Dietz Rago et al.

Environmental Research Letters



PAPER

OPEN ACCESS

RECEIVED
2 March 2020

REVISED
19 August 2020

ACCEPTED FOR PUBLICATION
26 August 2020



PUBLISHED
12 October 2020

Original content from this work may be used under the terms of the [Creative Commons Attribution 4.0 licence](https://creativecommons.org/licenses/by/4.0/).

Any further distribution of this work must maintain attribution to the author(s) and the title of the work, journal citation and DOI.



The bioclimatic extent and pattern of the cold edge of the boreal forest: the circumpolar taiga-tundra ecotone

Paul M Montesano^{1,2} , Christopher S R Neigh¹, Matthew Macander³ , Min Feng⁴ and Praveen Noojipady^{1,2}

¹ Code 618, Biospheric Sciences Laboratory, NASA Goddard Space Flight Center, Greenbelt, MD 20771, United States of America

² Science Systems and Applications, Inc., 10210 Greenbelt Road, Lanham, MD 20706, United States of America

³ ABR, Inc.—Environmental Research & Services, 2842 Goldstream Road, Fairbanks, AK 99709, United States of America

⁴ TerraPulse, Inc., 13201 Squires Ct, North Potomac, MD 20878, United States of America

E-mail: paul.m.montesano@nasa.gov

Keywords: ecotone, boreal, forest, taiga, tundra, structure, landscape, pattern, tree, canopy, cover, circumpolar, biome, boundary

Supplementary material for this article is available [online](#)

Abstract

Current configurations of forest structure at the cold edge of the boreal may help understand the future of ecosystem functioning in high northern latitudes. The circumpolar biome boundary at the boreal (taiga) forest and tundra interface is an ecological transition zone (taiga-tundra ecotone; TTE) experiencing changes that affect its forest structure. We accounted for the TTE's horizontal forest structure with an estimate of its extent and pattern as represented by tree canopy cover (TCC). We quantified TCC patterns with an algorithm that describes its spatial gradient, and summarized landscape patterns of structure to represent heterogeneity, capturing abrupt, diffuse, and uniform forest at mesoscales. We used these landscape patterns to constrain the spatial extent of sparse and open canopy forest, and non-forest (forest-adjacent) edge that defines the TTE extent. The resulting map of the TTE extent is based on forest structure spatial patterns resolved at 30 m, highlights structural variability across landscapes, and helps distinguish tundra from boreal domains. We classified 14 594 landscapes as those associated with the TTE within a circumpolar bioclimatic envelope (11.575 million km²), where 44.83% of the area of these landscapes were forest and non-forest edge, yet 36.43% contributed to the TTE extent. We report the overall extent of the TTE (3.032 million km²) across North America and Greenland (53%), and Eurasia (47%), where 0.697 million km² is non-forest edge, 0.549 million km² is sparse forest, and 1.787 million km² is open canopy forest. Diffuse forest landscapes dominate the TTE (79%), and abrupt landscapes (~19%) indicate portions of the TTE where sparse forest and non-forest edge are the prevailing structural patterns. This account of the TTE quantifies the area of the cold edge of the boreal forest where previous global estimates show high discrepancies, and can help target monitoring and prediction of circumpolar dynamics.

1. Introduction

At the northern forest limit, the biome boundary between boreal (taiga) forest and tundra, the taiga-tundra ecotone (TTE; also referred to as the FTE) is recognized for its patchy gradient of woody vegetation [1, 2]. Here, the structure of this vegetation is typically in the form of short trees, tall shrubs or some spatial arrangement of the two across a range of canopy cover, and at coarse scale is associated with the mean July isotherm of 10 °C–12 °C [3–6].

The general reduction in height, cover, density, and above-ground biomass in this structure across a temperature gradient (both latitudinally and altitudinally) forms a transition zone from forested to tundra landscapes at the cold edge of the boreal forest.

The current structure and arrangement of woody vegetation in this transition zone are linked to a range of biophysical and biogeochemical patterns and processes in and near the high northern latitudes (>60° N). These include climate [7], fire patterns [8, 9], below-ground carbon and permafrost stability

[10–13], seed dispersal [14], stand age and carbon accumulation [15], and albedo [16, 17]. Insights into the relative strengths of static (e.g. photoperiod) and shifting (e.g. air temperature) drivers of the TTE provide guidance for how TTE changes continue to be monitored [18]. Model-based predictions of changes suggest continued structural growth and productivity increases with warming temperatures where current woody structure growth in the TTE is controlled primarily by climate [19]. However, identifying where (and at which scales) such primary controls operate may be key to accurately predicting TTE dynamics [20, 21]. The variability in primary controls and the likelihood and pattern of structural changes are important characteristics in and near this biome boundary because they modify ecosystem properties that govern how the land surface affects dynamics such as fluxes in trace gases, water, and energy, at seasonal, yearly, and decadal time scales [22, 23]. Thus, observations of the various configurations of woody structure with remote sensing may provide a means for inferring the fate of structure itself, the biome boundary that it demarcates, and the biophysical and biogeochemical processes to which this structure is linked.

Satellite observations of ecological boundaries are often uncertain for a variety of reasons. First, they are difficult to precisely demarcate, often manifesting as a gradient of vegetation patches [24, 25]. This spatial uncertainty is a prominent trait of the TTE, and as such there is an inherent scale dependency associated with its detection [1, 26, 27]. Second, institutional definitions of what constitutes a ‘forest’ often reflect lower latitude expectations for temperate and tropical forest structure [28]. For example, tree cover >30% satisfies the United Nations Framework Convention on Climate Change’s conservative definition of a forest, but excludes important TTE landscapes where forests are important for landscape structure and function. Third, shrubs serve a similar biophysical role as trees in the TTE when they are tall enough to emerge above accumulated snow [29], yet are often not recognized as part of a conventional forested extent. Landsat-derived maps do not reliably distinguish between shrubs and trees, and are likely to include shrubs with sparse forest extents [30, 31]. These tree cover criteria for forests, coupled with the uncertainty of identifying boundary forests from satellite data, confound the spatial delineation of this circumpolar biome boundary, potentially affecting accurate accounting of decadal-scale changes in surface albedo, permafrost carbon storage, and vegetation structure change [32–34].

To address these issues related to boundary detection, a hierarchical geospatial framework is useful because it links characteristics across scales [35, 36]. Within this hierarchical framework, a gradient-based

approach can provide a means to quantify patterns associated with gradual and abrupt changes across landscapes [37, 38]. This helps to resolve gradients at relevant spatial scales, which is useful because the measurement of gradients can change with scale [39], and inappropriate scales of analysis may not resolve spatial gradients of interest.

As climate changes, there exists an urgency in accounting for forest structure gradients. Studies recognize the importance of forest ecotones when examining drivers of current structure and changes (both underway and forthcoming) [35, 40–47]. Forest structure can be represented vertically (e.g. relative canopy heights) and horizontally (e.g. canopy cover) [48]. The gradient of structure may help understand variations in growth [49–52] establishment [53], and reproductive potential [54, 55]. Ground observations across the TTE suggest these gradients are a result of many factors [43, 49, 56–59]. For example, abrupt gradients (rapid spatial changes) of structure may be decoupled from climate, and more closely linked to site hydrology and soil thermal properties [60, 61]. The factors driving these structure gradients are associated with site history of land use, disturbance and rates of regrowth, herbivory, climate, proximity to oceans, and site conditions associated with topography, hydrology, permafrost, snow accumulation, soil, bedrock, wind, and seed availability, germination, and survival [62–64]. Pattern provides information on process, and current local-scale TTE structural gradients may be important for understanding the variation in primary factors controlling the TTE.

The identification of these TTE forest structure patterns at site scales across a broad domain in a standardized manner is challenging yet important. This pattern identification is a step towards understanding the overall processes of change, their causes and consequences, and the vulnerability of current structure and landscapes to shifts towards novel configurations of tree cover, density, height, deciduousness, and productivity. Earlier work [31, 65–71] assessed the extent of the TTE by applying a variety of gradient- and texture-based approaches to delineate structure, often recognizing the need for the consistent circumpolar application of these approaches [40, 72]. A common goal of many of these efforts was to identify the extent of the biome boundary while also capturing the variability of its forest structure. Problems with scale, such as the inability to resolve sparse tree cover, have hampered understanding of this variability, and the causes and consequences of ecotone change [73]. These scaling issues also restrict the recognition of overall forest area based on tree cover criteria and satellite uncertainty [28]. Here, we present work that combines broad-scale modeled climate, ecological region delineations,

mesoscale landscapes, and local-scale forest structure to quantify the extent and assess forest structure patterns of the circumpolar TTE.

2. Methods

2.1. Deriving a bioclimatic envelope to identify the taiga-tundra ecotone

To identify the extent and pattern of forest structure in the TTE we compiled a geographic envelope spanning the climatic gradients present across warm tundra and cold boreal forest landscapes. This envelope was used to constrain the analysis of tree canopy cover (TCC) and its gradient to where these forest structure characteristics are likely to be associated with the taiga-tundra biome boundary and not forest-steppe or unmanaged-managed land cover transitions, and to account for broad scale temperature control of the TTE.

To help identify this coarse climatic extent, we used the southern limit of the Arctic tundra as defined by the circumpolar arctic vegetation map (CAVM) [74, 75] to approximate the northernmost limit of trees. The CAVM treeline served as a rough spatial guide around which we extended a ‘cold’ domain (generally northward) and a ‘warm’ domain (generally southward) using the mean temperature of the warmest quarter (June–August) from the WorldClim (Version 2) set of modeled bioclimatic variables [76]. We used a temperature range $>7^{\circ}\text{C}$ and $<14^{\circ}\text{C}$ to incorporate landscapes known to support microsite boreal forest refugia in the ‘cold’ portion of the envelope, and extended the ‘warm’ portion southward to include most of the Hudson Plains [1]. Within both Nearctic (North America, including Greenland) and Palearctic (Eurasia) realms we used the ‘taiga’ and ‘tundra’ portions of the World Wildlife Fund’s terrestrial ecoregions [77] as a secondary coarse scale mask to constrain the southern limits of the bioclimatic envelope. This mask primarily reduced the area included in this envelope in the southern Siberian Sayan and Altai Mountains, limited the domain to the coastal ranges of southeastern Alaska, and removed portions of mid-latitude Ontario and Quebec. Finally, we applied a satellite-based (Landsat) water mask [78] to reduce the domain to land surface, and excluded all areas south of 50°N . A satellite-based TCC composite map was assembled within this coarse bioclimatic envelope.

2.2. Assembling a circumpolar satellite-based tree canopy cover composite

We assembled a satellite-based TCC composite using data derived from 30 m resolution multi-spectral measurements of vegetation from Landsat to account for horizontal forest structure. We combined two contemporaneous TCC products derived from work described in Montesano *et al* 2016 [31], Sexton *et al*

2013 [28], and Hansen *et al* 2013 [79]. This composite nominally represented TCC for year 2010 within the TTE domain, which spans parts of the two biogeographic realms. In the Nearctic, we used TCC data that was calibrated to represent woody vegetation canopies greater than 2 m in height [30, 31]. In the Palearctic, we used TCC from Hansen *et al* [79], which more clearly represents the woody vegetation gradient in open canopies across Siberia (figures S3, S4, S5 (available online at stacks.iop.org/ERL/15/105019/mmedia)). To temporally harmonize these data, we applied a mask to TCC from Hansen *et al* to exclude pixels showing forest loss before 2010. We then finalized the circumpolar composite by re-gridding (using nearest neighbor) the Palearctic TCC to match the TCC data in the Nearctic. Landsat-derived maps of vegetation structure often have high pixel-level uncertainty ($\sim\pm 30\%$ TCC), tend to overestimate cover in sparse forests, do not distinguish shrubs from trees, and thus feature noisy representations of all woody vegetation often influenced by the presence of non-woody vegetation at and near the ground level [31]. Yet, the patterns formed by groups of adjacent pixels in these composites introduce important and underutilized forest structure spatial context that mitigates the average uncertainty of any single pixel alone.

2.3. Refining tree canopy cover in the bioclimatic envelope

We applied a water occurrence mask to identify tree cover adjacent to sites where standing water has occurred, and reclassified tree cover to 0 where water was mapped with a frequency of $\geq 1\%$. This assumed that tree cover is not present in areas inundated at least 1% of the time between March 1984 and October 2015 [80]. This assumption is supported by the fact that the global water estimates are based on Landsat data that are unlikely to identify water underneath forest canopy. Furthermore, infrequently inundated vegetation is often below the 2 m canopy height threshold for trees that formed the basis for determining TCC. Therefore, this step served as a refinement to our tree cover estimates near water, mitigating the tendency for the overestimation of TCC in areas dominated by non-woody vegetation.

2.4. Calculating abruptness: the spatial gradient of tree canopy cover

We calculated the local spatial gradient in TCC (abruptness) from the Landsat TCC composite across the domain to quantify the uniform, diffuse, or abrupt nature in the change of tree cover across space. The calculation uses the magnitude of TCC ranging from 0 to 100 ($magnitude_{TCC}$, %) and the spatial rate of change (local gradient, 4-connected neighbors, rescaled from $0-90^{\circ}$ to $0-100^{\circ}$) in TCC ($spatial_rate_of_change_{TCC}$), and was calculated on a

per-pixel basis as such (Equation (1)):

$$\begin{aligned} \text{abruptness}_{TCC} &= (\text{spatial_rate_of_change}_{TCC} - \text{magnitude}_{TCC}) / \\ &(\text{spatial_rate_of_change}_{TCC} + \text{magnitude}_{TCC}) \end{aligned} \quad (1)$$

Equation (1) provides a normalized spatial rate of change that is not sensitive to the magnitude of tree cover with a unitless range from -1 to 1 . Therefore, sparse extents of tree cover with consistent values can have the same measure of uniformity as dense extents of tree cover. The result is a continuous set of values whose endmembers describe a uniform forest ($\text{abruptness}_{TCC} = -1$), where there is no difference in the tree cover value of a pixel and any values of its neighboring pixels and where $\text{magnitude}_{TCC} > 0$) or abrupt forest ($\text{abruptness}_{TCC} = 1$, $\text{magnitude}_{TCC} = 0$), indicating where a non-forested pixel is adjacent to a pixel with $\text{magnitude}_{TCC} > 0$. The mid-point along this continuum describes a gradual gradient used to identify diffuse forest.

2.5. Assessing the TTE extent: classifying and quantifying TTE forest structure and pattern across pixels and landscapes

We assessed *TTE extent*, the extent of non-forest edge, sparse, and open canopy forest that constitutes the TTE, using the bioclimatic envelope and predominant patterns of pixel-level forest structure across landscapes. We built a 30 m scale forest structure pattern classification map to quantify the extent of the TTE and its forest structure patterns with a series of steps to stratify, classify, and combine the magnitude_{TCC} and gradient of tree cover (abruptness_{TCC}) in the bioclimatic envelope (figure S1). Table 1 shows the forest structure pattern class matrix, described below, that was used to derive the 11 classes describing the pattern of forest structure for each pixel in the bioclimatic envelope.

We stratified magnitude_{TCC} into general zones to describe the *sparse* portion of the TTE (1–5% tree cover), the *open* canopy portion (6–30% tree cover), and an *Intermediate and Closed* canopy extent (>30% tree cover). The 30% tree cover cutoff is a convention [20] that accommodates a variety of forest transitions in the domain, a point of inflection in the accuracy of visual estimates of TCC [81], and approximates the magnitude of pixel-level uncertainty in boreal TCC estimates [31]. Therefore, this limit was inclusive, in that it allowed our analysis to extend further into open canopy boreal forest, which can be important parts of the TTE (e.g. dense patches of microsite forest refugia, riparian bands of forest, etc.). We accounted for the more dense forest structure of the ‘*Intermediate-Closed*’ classes to retain knowledge of forest structure within the broader bioclimatic envelope that was likely not associated with the TTE itself.

We stratified the abruptness_{TCC} values to describe six gradient classes, four of which are *uniform*, *diffuse-gradual*, *diffuse-rapid*, and *abrupt*. The remaining set of pixels represent the non-forest edge of forest structure where $\text{magnitude}_{TCC} = 0$ and $\text{abruptness}_{TCC} = 1$. This non-forest edge set was divided into 2 classes using the water mask described above, identifying non-forested pixels where water occurs (*non-forest edge_{water}*), or does not (*non-forest edge_{land}*).

We identified TTE landscapes using the proportions of their forest structure pattern classes within spatial bounds determined by hydrological basins [82]. Landscapes were bounded using level 8 (landscape) hydrobasins, and were nested within level 1 (circumpolar regions) hydrobasins, and biogeographic realms (Nearctic, Palearctic) that intersected the bioclimatic envelope of the TTE. These hydrological basins were a means to introduce basic topographic stratification to the classified pixels. The median size of the landscape hydrobasins used in this study was 388.7 km² (figure S2) and describe ‘meso-scale’, referenced hereafter.

For each landscape intersecting the bioclimatic envelope, we created a ‘landscape pattern class’ by grouping its forest structure patterns according to general gradient categories. To do this, we used the pixels with a forest structure pattern class described in table 1 following the schema diagrammed in figure 1. The result was a landscape pattern classification that defined ‘*TTE landscapes*’, whose forest structure patterns were used to derive the ‘*TTE extent*’. We also identified a subset of these landscape hydrobasins that intersected the circumpolar arctic vegetation map (CAVM) treeline to examine the forest structure patterns across a subset of the TTE bioclimatic extent that coincides with a representation of the northernmost extent of trees, a widely used demarcation between the arctic and boreal vegetation domains.

3. Results

3.1. The bioclimatic envelope that contains the taiga-tundra ecotone

The bioclimatic envelope in which the TTE exists is a large spatial margin (11.575 million km²) that encapsulates portions of warm tundra and cold boreal domains (figure 2). The envelope extends across part or all of six broad circumpolar regions, and includes sites at the northernmost ranges of the boreal forest where recent studies have documented a variety of climate-induced changes to forest structure [5, 59, 83–91].

3.2. The extent and pattern of the taiga-tundra ecotone

3.2.1. The extent and pattern of forest structure in the bioclimatic envelope

Across North America (which hereafter includes Greenland) and Eurasia this bioclimatic envelope has

Table 1. The forest structure pattern classification matrix showing 11 pixel-level classes formed from the combination of the gradient and magnitude of tree canopy cover. Bold text identifies forest structure pattern classes. Gradient classes are stratifications of the range of $abruptness_{TCC}$ and magnitude classes are a stratification of $magnitude_{TCC}$. The two pattern classes for which $tcc = 0$ represent land adjacent to forest and indicates whether water does ($non\text{-}forest\ edge_{wet}$), or does not ($non\text{-}forest\ edge_{dry}$), occur.

		Magnitude classes of tree canopy cover (tcc, %)			
		$tcc = 0$	$0 < tcc \leq 5$	$5 < tcc \leq 30$	$tcc > 30$
Gradient classes of tree canopy cover (<i>a</i> , unitless)	<i>Null</i>	<i>Non-forest</i>	<i>Forest</i>		
	$-1 \leq a \leq -0.5$		Sparse and uniform	Open and uniform	
	$-0.5 < a \leq 0$		Sparse and diffuse-gradual	Open and diffuse-gradual	
	$0 < a \leq 0.5$		Sparse and diffuse-rapid	Open and diffuse-rapid	Intermediate
	$0.5 < a < 1$		Sparse and abrupt	Open and abrupt	—Closed
	$a = 1$	Non-forest edge (dry)			
	$a = 1, water\ occurs$	Non-forest edge (wet)			

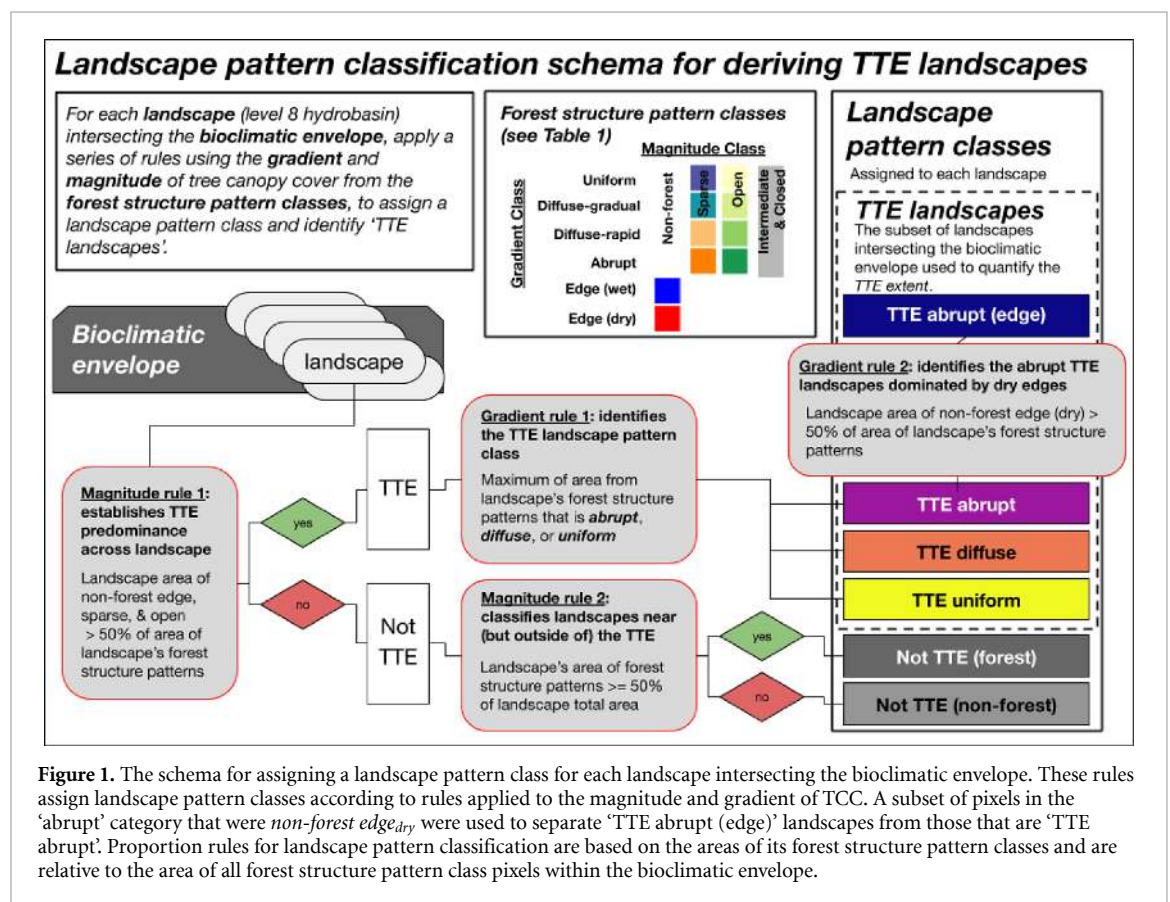


Figure 1. The schema for assigning a landscape pattern class for each landscape intersecting the bioclimatic envelope. These rules assign landscape pattern classes according to rules applied to the magnitude and gradient of TCC. A subset of pixels in the 'abrupt' category that were $non\text{-}forest\ edge_{dry}$ were used to separate 'TTE abrupt (edge)' landscapes from those that are 'TTE abrupt'. Proportion rules for landscape pattern classification are based on the areas of its forest structure pattern classes and are relative to the area of all forest structure pattern class pixels within the bioclimatic envelope.

an extent of forest and non-forest edge that accounts for 62.5% (7.24 million km²) of the envelope's land surface (figure 3). Landscape-scale proportions of this extent indicate a gradient of forest structure (figure 4). In this envelope across Eurasia, more than half (57.83%) of this forest is >30% TCC, while sparse and open canopies dominate the forest portion of this envelope in North America (84.74%). The non-forest edge and sparse and open canopy forest portions account for 33.57% of the envelope (>3.888 million km²). A subset of this area, when further constrained by mesoscale landscape patterns, defines the TTE extent.

3.2.2. Mesoscale landscape patterns that constrain the taiga-tundra ecotone

figure 5(a) and (b) presents a landscape pattern classification of landscapes intersecting the bioclimatic envelope. Figure 5(a) shows the area of the forest structure patterns (non-forest edge, sparse, and open canopy forest) that determine the landscape patterns and figure 5(b) maps these landscapes. The landscape pattern classification imposed a mesoscale constraint on the total extent of non-forest edge, and sparse and open canopy forest that we associate with the TTE. In the bioclimatic envelope, a total of 26 566 landscapes were classified. Landscapes associated with the TTE

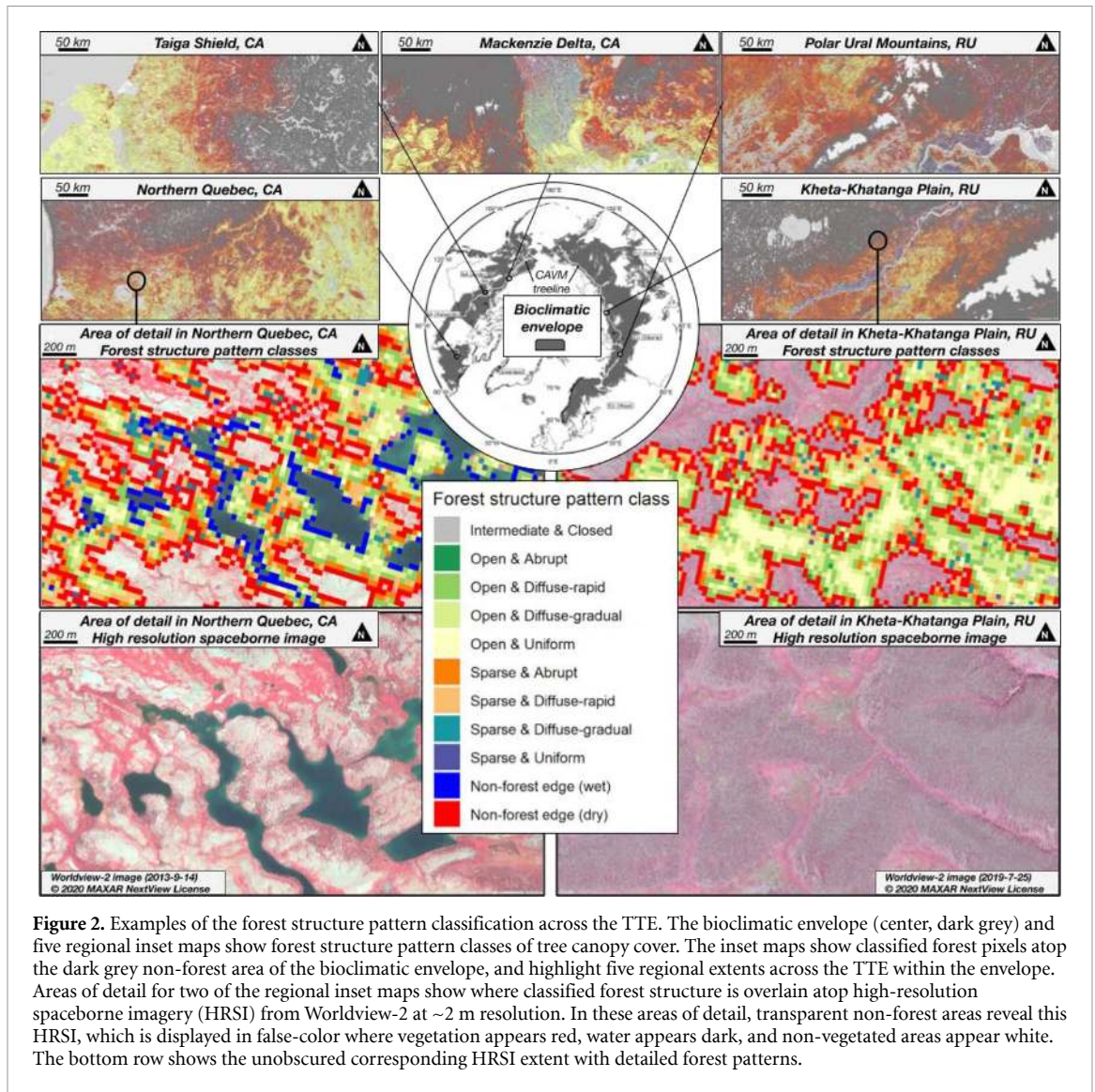


Figure 2. Examples of the forest structure pattern classification across the TTE. The bioclimatic envelope (center, dark grey) and five regional inset maps show forest structure pattern classes of tree canopy cover. The inset maps show classified forest pixels atop the dark grey non-forest area of the bioclimatic envelope, and highlight five regional extents across the TTE within the envelope. Areas of detail for two of the regional inset maps show where classified forest structure is overlain atop high-resolution spaceborne imagery (HRSI) from Worldview-2 at ~2 m resolution. In these areas of detail, transparent non-forest areas reveal this HRSI, which is displayed in false-color where vegetation appears red, water appears dark, and non-vegetated areas appear white. The bottom row shows the unobscured corresponding HRSI extent with detailed forest patterns.

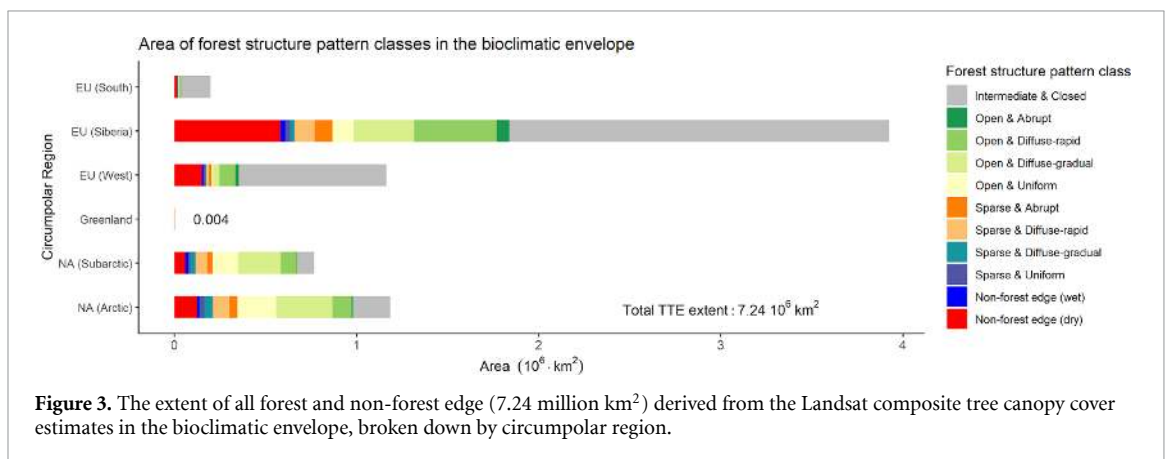


Figure 3. The extent of all forest and non-forest edge (7.24 million km²) derived from the Landsat composite tree canopy cover estimates in the bioclimatic envelope, broken down by circumpolar region.

(TTE landscapes, 14 594) cover 8.323 million km², where 44.83% of the area of these landscapes are associated with forest $\leq 30\%$ tree cover and edge. However, only a portion of these TTE landscapes were non-forest edge, and sparse and open canopy forest that contribute to the extent of the TTE, as discussed below.

3.2.3. The TTE extent across classified landscapes
 The TTE extent is the areal combination of the forest structure pattern classes representing tree cover $\leq 30\%$ that are found in TTE landscapes. This TTE extent in these TTE landscapes has a total area of 3.032 million km², or 26.2% of the envelope, and 36.43% of the TTE landscapes.

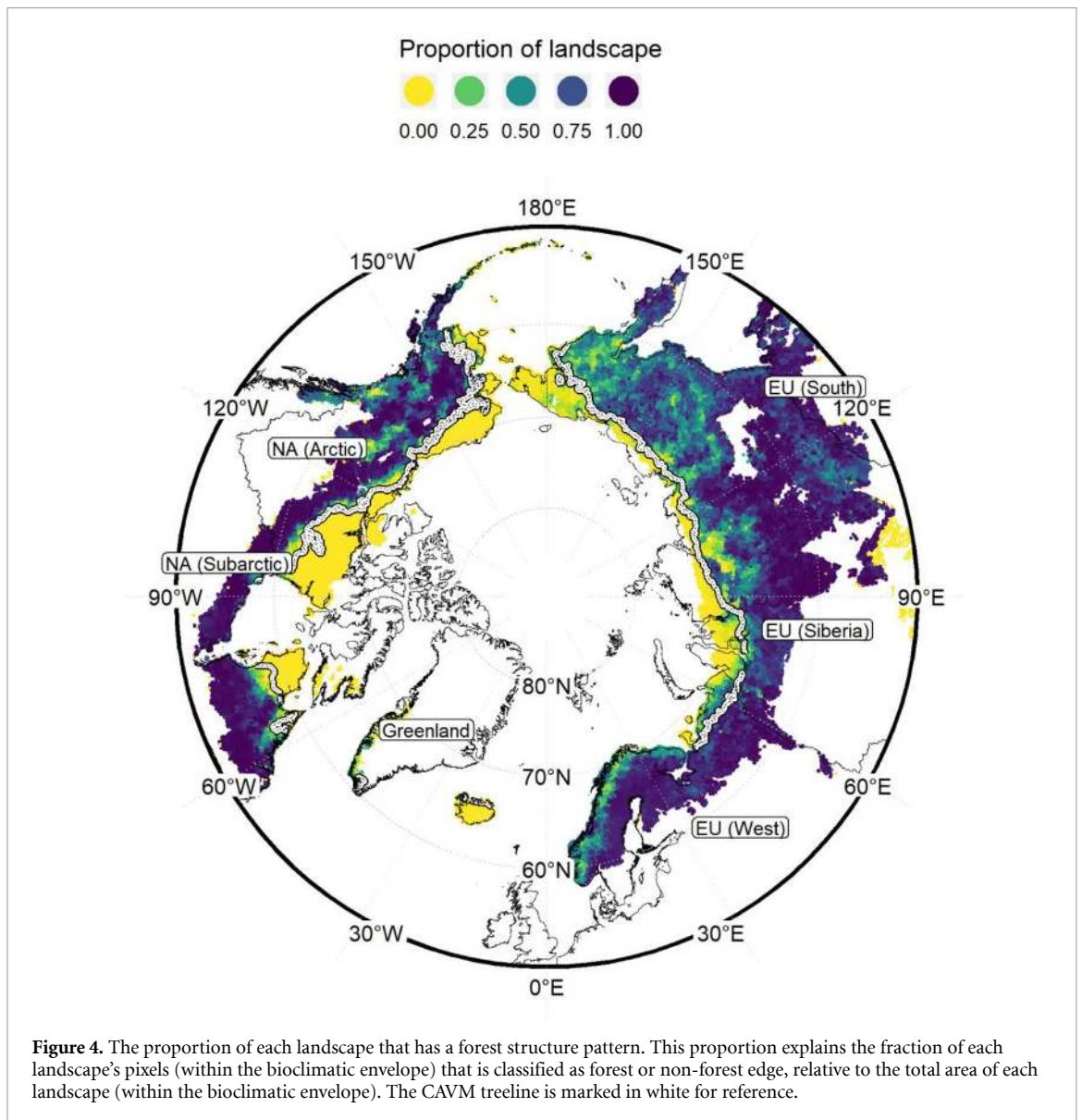
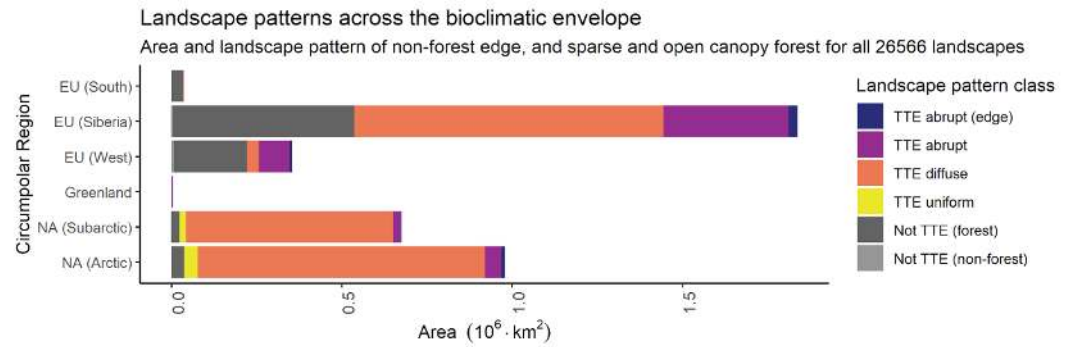


Table 2 (and figure S6) further summarizes the *TTE extent* across *TTE landscapes*. Of the *Forest* and *Non-forest (edge)* portions associated with the *TTE extent*, those which are nested within a broader landscape pattern of *TTE diffuse* account for 79% of the *TTE extent*, followed by *TTE abrupt* (17.51%), *TTE uniform* (1.92%), and *TTE abrupt (edge)* (1.57%). The total forested component of the *TTE extent* is 2.335 million km², representing 77.01% of the *TTE extent*.

Additionally, table 2 reports prominent differences between the *TTE extent* across the two circumpolar biogeographic realms. First, the Nearctic (North America, Greenland) accounts for the majority of the *TTE extent* (52.63%). This is in part due to the greater proportion of *Intermediate and Closed* canopies accounting for forest area in bioclimatic envelope in the Palearctic. Second, in North America,

the *TTE extent* occupies primarily the southern portion of its bioclimatic envelope, where the Brooks Range and Canadian Shield are associated with the northernmost limits of its extent. In contrast, the *TTE extent* in Eurasia approaches the northern limits of the bioclimatic envelope, particularly across Siberia. Here, the coupled permafrost-larch forest system accounts for forest structure that achieves the northernmost limits of forest growth. Third, the *TTE extent* across *TTE abrupt (edge)* landscapes (figure 4) is 0.014 million km² in North America, 0.033 million km² in Eurasia, and accounts for 1.57% of all *TTE extent*. Yet, these landscapes are distributed conspicuously across the northern edge of the bioclimatic envelope in Siberia, and to a lesser extent the North American subarctic. A prominent subset of this extent is the forest-adjacent (but unforested) *non-forest edge_{dry}*. This portion of the *TTE*, which helped

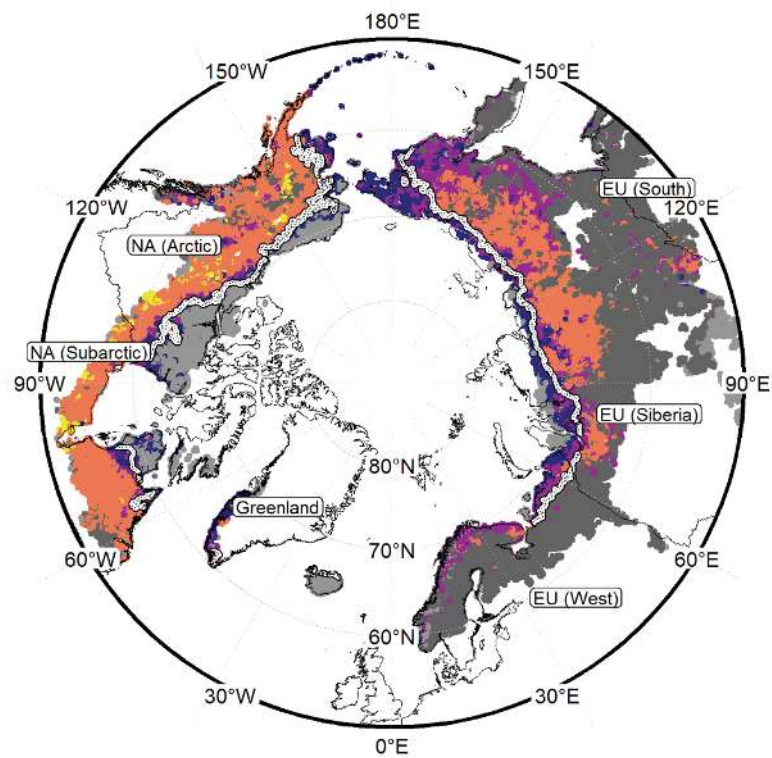


(a)

Landscape patterns across the bioclimatic envelope

Colored pattern classes identify the 14594 landscapes used to define the TTE extent

Landscape pattern class



(b)

Figure 5. (a) Bar plots of the area of the forest structure patterns (*non-forest edge*, *sparse*, and *open canopy forest*) that determine the landscape patterns across the six circumpolar regions. (b) The corresponding map of landscape patterns of forest structure across the circumpolar bioclimatic envelope overlain with CAVM treeline as reference. This classification of landscapes based on their prevailing forest structure is a mesoscale constraint on the area of forest structure used to determine the extent of the taiga-tundra ecotone.

Table 2. The TTE extent ($3.032 \times 10^6 \text{ km}^2$) and pattern (landscape pattern class) across the 2 circumpolar biogeographic realms for the forest and non-forest (edge) portions.

Landscape pattern class	Nearctic			Palearctic			Sub-total			Total	
	Forest (km ²)	Non-forest (edge) (km ²)	Forest (km ²)	Non-forest (edge) (km ²)	Forest (km ²)	Non-forest (edge) (km ²)	Forest (km ²)	Non-forest (edge) (km ²)	Forest (km ²)	Non-forest (edge) (km ²)	%
TTE abrupt (edge)	5714	8465	12508	20887	18221	29352	18221	29352	18221	29352	0.60
TTE abrupt	40235	32284	241127	217332	281362	249615	281362	249615	281362	249615	9.28
TTE diffuse	1278942	172047	700140	244416	1979082	416463	1979082	416463	1979082	416463	65.27
TTE uniform	56597	1657	–	–	56597	1657	56597	1657	56597	1657	1.87
Total	1381487	214452	953774	482634	2335262	697087	2335262	697087	2335262	697087	77.01
%	45.56	7.07	31.45	15.92							
Total: realms	1595940			1436409							
%: realms	52.63			47.37							
					Total TTE extent (km ²):				3032348		

define the abrupt portions of the TTE, accounts for 22.99% of the total *TTE extent*, of which 15.92% is in Eurasia.

3.3. The variability of forest structure patterns across TTE landscapes

The variability of forest structure patterns of the *TTE extent* are shown in figure 6. For all 14 594 *TTE landscapes* they summarize the final pixel-level results, reveal differences in the forest structure patterns used to classify landscapes across each circumpolar region, and highlight the variability in forest structure representation within and between North American and Eurasian landscapes. The difference in *non-forest edge_{dry}* proportions between the two circumpolar realms is the most prominent source of variability in TTE pattern. In Eurasia, 62% of TTE landscapes are 25% *non-forest edge_{dry}*, in contrast to 36% in North America. For the subset of *TTE landscapes* that intersect the CAVM treeline, this figure shows that there is greater consistency in forest structure pattern across this portion of the circumpolar TTE than across the broader, more variable, full TTE extent. These 1061 landscapes encapsulate a portion of the TTE that is associated with particularly sparse forest structure near the northern limit of the TTE extent in the bioclimatic envelope. Of this subset of CAVM landscapes in the TTE, 818 (77%) are either *TTE abrupt (edge)* or *TTE abrupt*. The landscapes where *non-forest edge_{dry}* dominate the within-landscape pattern suggest where forest structure is most discontinuous, and where they be most uncertain.

4. Discussion

4.1. A new account of a global biome boundary in the high northern latitudes

These results present a new account of the extent and pattern of the circumpolar TTE circa 2010, a global scale land cover transition between the boreal and tundra domains in the high northern latitudes. The TTE is contained within a broad scale bioclimatic envelope, and is constrained by mesoscale prevalence of the patterns in the magnitude and gradient of forest structure that are resolved at 30 m. It forms a broad geographic band in which forest structure patterns indicate a transition from primarily diffuse to abrupt forest gradients across the boreal-tundra biome boundary. The preponderance of landscapes with abrupt patterns of forest structure indicates the limits of woody structure, which likely include extensive dense shrublands.

These results, at a practical level, enable TTE studies to account for forest structure pattern and its spatial variation. These patterns update existing TTE spatial information that is represented with linear features (e.g. treelines) [74, 75] and coarse tree cover patches [67]. The pixel-level patterns and the

mesoscale landscape summaries quantify forest features in the TTE at local, regional, and circumpolar scales. This TTE representation is important because it reveals forest gradients in all directions, useful for identifying detailed east-west gradients linked to local disturbance patterns, and soil and topographic conditions, and complexities in vegetation greening [92, 93]. These gradients may in part explain the causes of current vegetation patterns and help predict vulnerability to change, ultimately helping assess a variety of forest structure and tundra vegetation changes in the TTE, beyond just the northward advance of woody vegetation.

This gradient-based representation reveals and quantifies a broad biome boundary with large extents of diffuse forest structure landscapes, and identifies landscapes where abrupt forest gradients represent areas of frequent disruption of forested extents. This map shows that while these ‘abrupt’ landscapes do not have extensive forest structure (<20% of the overall *TTE extent*), the non-forested edges with sparsely forested sites may indicate priority monitoring and prediction sites to target with high resolution remote sensing [94]. These abrupt and edge subsets of the TTE will provide the spatial bounds for closely examining detailed changes in vegetation structure near the limits of vertical tree growth forms for all of its circumpolar sub-domains. Furthermore, this gradient-based TTE extent may provide useful prior information on seed availability to individual-based models that incorporate seed dispersal routines to predict TTE changes [95].

These results highlight the variability of TTE forest structure to elevate its importance for studying TTE change. This variability, quantified and illustrated in multiple ways in this study (particularly in figures 4, 5(b) and 6), is useful for identifying structurally similar TTE landscapes. Whether spatially adjacent or disparate, similar landscapes can provide a starting point for understanding the fate of different parts of the TTE, and its variability will be important prior information for tracking ongoing, and predicting upcoming changes. Divergence in the change trajectories of structurally similar TTE landscapes may illustrate differences in how forest structure responds, ultimately, to warming.

4.2. Targeting priority sites for circumpolar monitoring and prediction using the TTE extent

The TTE extent provides a mesoscale lens that can be used to target priority sites in greater detail. In the TTE, where spaceborne estimates of forest structure have shown high discrepancies [28] this study’s proportional representation of forest structure patterns supports targeting of structurally uncertain landscapes in a standardized and spatially consistent manner, critical across such an extensive and heterogeneous domain [73, 75], and facilitates comprehensive monitoring with stratified, high-resolution remote

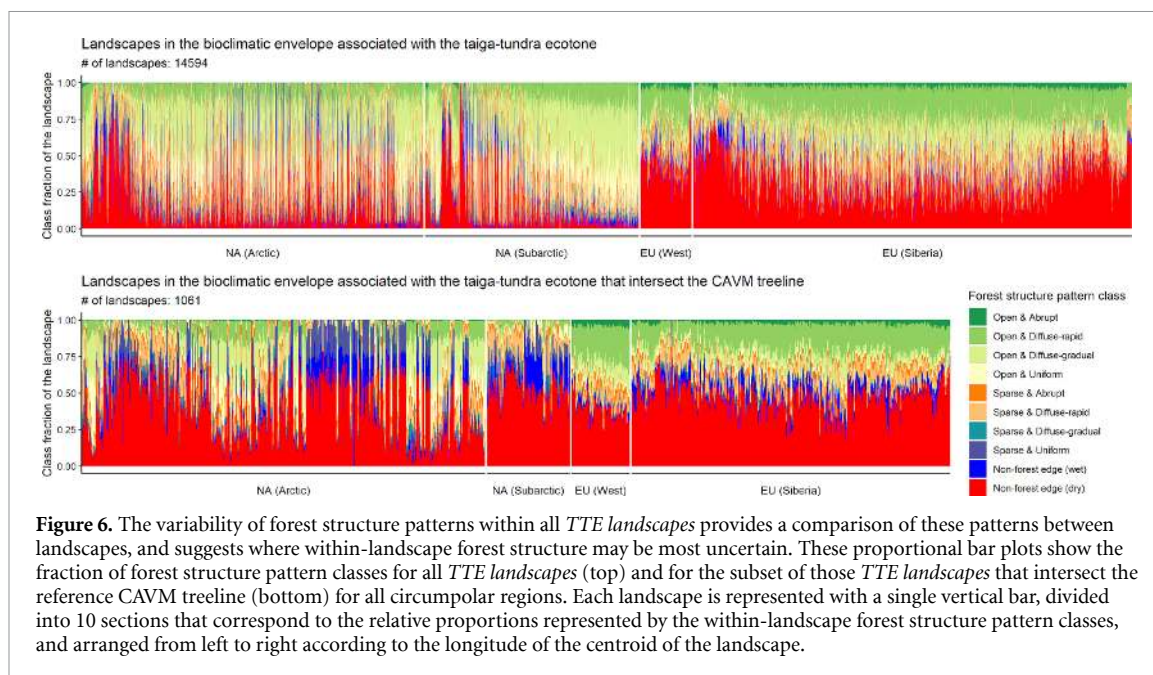


Figure 6. The variability of forest structure patterns within all *TTE landscapes* provides a comparison of these patterns between landscapes, and suggests where within-landscape forest structure may be most uncertain. These proportional bar plots show the fraction of forest structure pattern classes for all *TTE landscapes* (top) and for the subset of those *TTE landscapes* that intersect the reference CAVM treeline (bottom) for all circumpolar regions. Each landscape is represented with a single vertical bar, divided into 10 sections that correspond to the relative proportions represented by the within-landscape forest structure pattern classes, and arranged from left to right according to the longitude of the centroid of the landscape.

sensing or field-based sampling of circumpolar vegetation at various scales. This support of multi-scale monitoring may aid thorough explorations into the variation in vegetation structure [94], change [96, 97], flora-fauna interactions [98], climate feedbacks [17], and divergent or mixed structural and functional changes in vegetation [99, 100]. We retained the pixel-level classifications to assist with high resolution targeting, and to be able to refine landscape classification.

This TTE extent can also help target high resolution predictions for exploring their variability in light of current structure patterns. Spatially-explicit individual-based forest gap models [101–104] are suited for studying important forest structure changes at the cold boreal edge because, aside from those resulting from rapid disturbances (e.g. fire), woody structure changes at these latitudes often occur at magnitude and rates that challenge spectral-based change detection methods from current spaceborne time-series [105, 106]. Such models can integrate factors of change across all scales to model how the local expressions of change vary across broad extents. Yet, because these models run at high resolutions (individual tree level), they may be most effective when they are deployed with a stratified random sampling approach to build sets of predictions at various micro-sites that represent the range of ecologic conditions across the TTE. This TTE extent provides a practical means for identifying these micro-sites for high resolution modeling of likely variation in multi-decadal forest structure responses across the cold edge of the boreal.

Circumpolar monitoring with this TTE extent need not be limited to forest structure. For example, these maps may be used to: (a) identify a variety of warm tundra domains and update the CAVM tundra

extent, (b) provide a means for examining the interaction of permafrost and forests [107], (c) update uncertainties in canopy-snow interactions for snow-albedo feedback [108] and (d) can be coupled with paleo-environmental biomarkers [109] to build ecological identities of sub-districts within the arctic and sub-arctic. Such identities could be powerful prior input to predictions of biome boundary changes. Fundamentally, this TTE extent bounds a fairly indeterminate transitional environment to assist future studies in knowing where to look for changes across a vast domain.

4.3. Depicting the circumpolar TTE: an update to previous work, and sources of uncertainty

We updated previous work on the depiction of the circumpolar TTE by adopting a conceptual framework derived from studies that suggest forest structure patterns are relevant for examining temporal changes in the TTE [39, 45, 49, 110–112]. We note four primary guidelines of this framework as applied to forests along the cold edge of the circumpolar boreal:

- (a) forest structure is a fundamental feature used to define the ecotone,
- (b) a coupled areal- and gradient-based delineation of forest structure within the domain (instead of linear demarcation) acknowledges the indeterminate nature of the ecological transition zone itself and allows for flexible interpretation of it,
- (c) Mesoscale landscapes (e.g. hydrobasins) are part of a spatial hierarchy that serves as the basis for quantifying the spatial variability in the local patterns of forest structure, and representing differences across the domain.

- (d) Environmental factors at broad scales help constrain the domain to a bioclimatic envelope.

These guidelines provide a useful way of partially mitigating the effects of the pixel-level uncertainty of spaceborne forest structure estimates on TTE extent estimates.

The TTE is, by nature, an uncertain zone that eludes precise demarcation. Ecotones, conceptually, have indeterminate extents, thus the area results we present may change with a different set of rules and methods for the remote sensing of forest structure. These changes may arise from uncertainty in the sparse and open canopy forests of the TTE extent also arises from a mean pixel-level uncertainty of $\pm 30\%$ TCC from Landsat in boreal forests arising from overestimates of some sparse cover, discontinuities from data acquired from Landsat-7 after its scan-line corrector failed in 2003, and short seasonal windows for acquiring data in the TTE in northern Siberia [31].

For these reasons, the map's non-forest edge results may provide some measure of landscape-level uncertainty of the final estimates. For example, north-eastern Siberia features clustering of landscapes classified as TTE abrupt (edge) beyond known limits of tree cover. In these landscapes, in particular, the ratio of non-forest edge (dry) to actual forested area may suggest where noise in the estimate exceeds the signal of forest structure. Additional remote sensing data on surface topography and vegetation height, e.g. from HRSI or ICESat-2, will be an important complement to the magnitude and gradient of TCC for reducing large relative errors in forest structure across TTE extents at fine scales.

A detailed comparison with previous TTE delimitations was not the focus of this study. Given the inherent difficulty in defining geographic extents with indeterminate boundaries, comparisons are fraught with inconsistent definitions of features of interest. We note that the TTE extent from Ranson *et al* [66] covers 1.9 million km² (below 70° N) while this study estimates 2.335 million km² of forested TTE extent, and an additional 0.697 million km² of non-forest edge. This study's ~27% increase in the forested component of the TTE extent may be due to the consideration of more area (particularly in Eurasia), and the ability to resolve smaller and sparser forested areas.

This study of a broad-scale circumpolar domain and its heterogeneous landscapes benefited from a computational platform that facilitated a multi-scale analysis, whereby pixel-level estimates were transferred up to landscapes to mitigate some forest structure uncertainty [113]. Using this platform (Google Earth Engine), we accessed locally-scaled data (30 m pixels) and analyzed a forest gradient across ecological domains, incorporating biogeographic context from the proportional representation of forest

structure that emerged across landscapes. This platform helped address the need for a standardized protocol centered on the concept that the heterogeneity of forest structure across the TTE is based on estimates derived at spatial scales consistent with changes being examined [2, 71, 73].

5. Conclusions

These methods and results provide a new account of the extent and pattern of the circumpolar TTE that is contained within a broad scale bioclimatic envelope and constrained by mesoscale patterns in the magnitude and gradient of forest structure. The map of the TTE extent uses the spatial gradient of forest structure to quantify its variability across landscapes, to help distinguish tundra and boreal domains. We classify 14 594 landscapes as those associated with the TTE, covering 8.323 million km² within a circumpolar bioclimatic envelope (11.575 million km²), where 44.83% of that area of these landscapes are forest and non-forest edge pixels, yet 36.43% contribute to the TTE extent. The overall extent of the TTE is 3.032 million km² across North America and Greenland (53%) and Eurasia (47%), where 0.697 million km² is non-forest edge, and 2.335 million km² is forested (0.549 million km² is sparse forest, and 1.787 million km² is open canopy forest). Diffuse forest landscapes dominate the TTE accounting for 79% of its extent, and abrupt landscapes (~19%) indicate portions of the TTE extent where sparse and non-forest edge prevails. This multi-scale account of the TTE quantifies the area of the cold edge of the boreal forest where previous global estimates often show high discrepancies, and serves as a basis for closely examining ongoing changes in the heterogeneous circumpolar biome boundary.

Acknowledgments

This work was funded primarily by NASA grants NNH13ZDA001N-CARBON, NNH16ZDA001N-CARBON and NNH18ZDA001N-TE.

Data availability statement

The data that support the findings of this study are available upon reasonable request from the authors. The forest structure pattern classification and the bioclimatic envelope are available upon request as a Google Earth Engine asset, hydrobasins are available from www.hydrosheds.org. MAXAR data were provided by NASA's Commercial Archive Data for NASA investigators (cad4nasa.gsfc.nasa.gov) under the National Geospatial-Intelligence Agency's NextView license agreement.

Authors' contribution

PM conceived the study design, performed the analysis, and wrote the manuscript. CN helped with the study design and provided manuscript feedback. MF, PN, and MM assisted with analysis and provided manuscript feedback.

Conflict of interest statement

All authors declare no conflict of interest.

ORCID iDs

Paul M Montesano  <https://orcid.org/0000-0003-1695-2439>

Matthew Macander  <https://orcid.org/0000-0003-2808-208X>

References

- [1] Payette S, Fortin M-J and Gamache I 2001 The subarctic forest–Tundra: the structure of a biome in a changing climate *BioScience* **51** 709
- [2] Callaghan T V, Werkman B R and Crawford R M M 2002 The tundra–taiga interface and its dynamics: concepts and applications *Ambio Spec No* 12 6–14
- [3] Sveinbjörnsson B 2000 North American and European treelines: external forces and internal processes controlling position *AMBIO: J. Hum. Environ.* **29** 388
- [4] Epstein H E, Beringer J, Gould W A, Lloyd A H, Thompson C D and Chapin F S 2004 The nature of spatial transitions in the Arctic *J. Biogeogr.* **31** 1917–33
- [5] MacDonald G M, Velichko A A, Kremenetski C V, Borisova O K, Goleva A A and Andreev A A 2000 Holocene treeline history and climate change across northern Eurasia *Quat. Res.* **53** 302–11
- [6] Abaimov A P 2010 Geographical distribution and genetics of Siberian larch species *Ecol. Stud.* **41**–58
- [7] Macias-Fauria M, Forbes B C, Zetterberg P and Kumpula T 2012 Eurasian Arctic greening reveals teleconnections and the potential for structurally novel ecosystems *Nat. Clim. Change* **2** 613–8
- [8] Randerson J T et al 2006 The impact of boreal forest fire on climate warming *Science* **314** 1130–2
- [9] Rogers B M, Soja A J, Goulden M L and Randerson J T 2015 Influence of tree species on continental differences in boreal fires and climate feedbacks *Nat. Geosci.* **8** 228–34
- [10] Webb E E et al 2017 Variability in above- and belowground carbon stocks in a Siberian larch watershed *Biogeosciences* **14** 4279–94
- [11] Jorgenson M T, Harden J, Kanevskiy M, O'Donnell J, Wickland K and Ewing S 2013 Reorganization of vegetation, hydrology and soil carbon after permafrost degradation across heterogeneous boreal landscapes *Environ. Res. Lett.* **8** 035017
- [12] Takano S, Sugimoto A, Tei S, Liang M, Shingubara R and Morozumi T 2019 Isotopic compositions of ground ice in near-surface permafrost in relation to vegetation and microtopography at the taiga–tundra boundary in the Indigirka River lowlands, northeastern Siberia *PLOS One* **e0223720**
- [13] Berryman E, Ryan M G, Bradford J B, Hawbaker T J and Birdsey R 2016 Total belowground carbon flux in subalpine forests is related to leaf area index, soil nitrogen, and tree height *Ecosphere* **7** e01418
- [14] Johansson M E, Nilsson C and Nilsson E 1996 Do rivers function as corridors for plant dispersal? *J. Veg. Sci.* **7** 593–8
- [15] Alexander H D, Mack M C, Goetz S, Loranty M M, Beck P S A and Earl K 2012 Carbon accumulation patterns during post-fire succession in cajander larch (*Larix cajanderi*) forests of Siberia *Ecosystems* **15** 1065–82
- [16] Wang L, Cole J N S, Bartlett P, Versegny D, Derksen C and Brown R 2016 Investigating the spread in surface albedo for snow-covered forests in CMIP5 models *J. Geophys. Res.* **121** 1104–19
- [17] Loranty M M, Goetz S J and Beck P S A 2011 Tundra vegetation effects on pan-arctic albedo *Environ. Res. Lett.* **6** 024014
- [18] Eitel J U H, Maguire A J, Boelman N, Vierling L A, Griffin K L and Jensen J 2019 Proximal remote sensing of tree physiology at northern treeline: do late-season changes in the photochemical reflectance index (PRI) respond to climate or photoperiod? *Remote Sens. Environ.* **221** 340–50
- [19] Zhang W, Miller P A, Smith B, Wania R, Koenigk T and Döscher R 2013 Tundra shrubification and tree-line advance amplify arctic climate warming: results from an individual-based dynamic vegetation model *Environ. Res. Lett.* **8** 034023
- [20] Van Bogaert R, Haneca K, Hoogesteger J, Jonasson C, De Dapper M and Callaghan T V 2011 A century of tree line changes in sub-Arctic Sweden shows local and regional variability and only a minor influence of 20th century climate warming *J. Biogeogr.* **38** 907–21
- [21] Maguire A J, Eitel J U H, Vierling L A, Johnson D M, Griffin K L and Boelman N T 2019 Terrestrial lidar scanning reveals fine-scale linkages between microstructure and photosynthetic functioning of small-stature spruce trees at the forest-tundra ecotone *Agric. Forest Meteorol.* **269** 157–68
- [22] Bonan G B 2008 Forests and climate change: forcings, feedbacks, and the climate benefits of forests *Science* **320** 1444–9
- [23] Callaghan T V et al 2004 Effects of changes in climate on landscape and regional processes, and feedbacks to the climate system *Ambio* **33** 459–68
- [24] Risser P G 1995 The status of the science examining ecotones *BioScience* **45** 318–25
- [25] Arnot C, Fisher P F, Wadsworth R and Wellens J Landscape metrics with ecotones: pattern under uncertainty. *Landscape Ecology*. 2004. pp. 181–95. doi:land.0000021723.24247.ee
- [26] Fortin M-J 1999 Effects of quadrat size and data measurement on the detection of boundaries *J. Veg. Sci.* **10** 43–50
- [27] Fortin M-J, Olson R J, Ferson S, Iverson L, Hunsaker C and Edwards G 2000 *Landsc. Ecol.* **15** 453–66
- [28] Sexton J O, Noojipady P, Song X-P, Feng M, Song D-X and Kim D-H 2016 Conservation policy and the measurement of forests *Nat. Clim. Change* **6** 192–6
- [29] Loranty M M and Goetz S J 2012 Shrub expansion and climate feedbacks in arctic tundra *Environ. Res. Lett.* **7** 011005
- [30] Sexton J O, Song X-P, Feng M, Noojipady P, Anand A and Huang C 2013 Global, 30-m resolution continuous fields of tree cover: landsat-based rescaling of MODIS vegetation continuous fields with lidar-based estimates of error *Int. J. Digit. Earth* **427–48**
- [31] Montesano P, Neigh C, Sexton J, Feng M, Channan S and Ranson K 2016 Calibration and validation of Landsat tree cover in the taiga-tundra ecotone *Remote Sens.* **8** 551
- [32] Söderberg U, Wulff S and Ståhl G 2014 The choice of definition has a large effect on reported quantities of dead wood in boreal forest *Scand. J. Forest Res.* **1–29**
- [33] Siewert M B, Hanisch J, Weiss N, Kuhry P, Maximov T C and Hugelius G 2015 Comparing carbon storage of Siberian tundra and taiga permafrost ecosystems at very high spatial resolution *J. Geophys. Res.* **1973–94**
- [34] Blok D, Schaepman-Strub G, Bartholomeus H, Heijmans M P, Maximov T C and Berendse F 2011 The response of arctic vegetation to the summer climate: relation between

- shrub cover, NDVI, surface albedo and temperature
Environ. Res. Lett. **6** 035502
- [35] Malanson G P, Resler L M, Bader M Y, Holtmeier F-K, Butler D R and Weiss D J 2011 Mountain treelines: a roadmap for research orientation *Arct. Antarct. Alp. Res.* **43** 167–77
- [36] Case B S and Duncan R P 2014 A novel framework for disentangling the scale-dependent influences of abiotic factors on alpine treeline position *Ecography* **37** 838–51
- [37] Bowersox M A and Brown D G 2001 *Plant Ecol.* **89**–103
- [38] Moncrieff G R, Bond W J and Higgins S I 2016 Revising the biome concept for understanding and predicting global change impacts *J. Biogeogr.* **43** 863–73
- [39] Smith T M and Urban D L 1988 Scale and resolution of forest structural pattern *Vegetatio* **74** 143–50
- [40] Callaghan T V, Crawford R M M, Eronen M, Hofgaard A, Payette S and Rees W G 2002 The dynamics of the tundra-taiga boundary: an overview and suggested coordinated and integrated approach to research *Ambio* 3–5
- [41] Malanson G P, Resler L M and Tomback D F 2017 Ecotone response to climatic variability depends on stress gradient interactions *Clim. Change Responses* **4**
- [42] Dearborn K D and Danby R K 2017 Aspect and slope influence plant community composition more than elevation across forest-tundra ecotones in subarctic Canada *J. Veg. Sci.* **28** 595–604
- [43] Dearborn K D and Danby R K 2019 Spatial analysis of forest-tundra ecotones reveals the influence of topography and vegetation on alpine treeline patterns in the subarctic *Ann. Am. Assoc. Geogr.* 1–18
- [44] Trant A J, Lewis K, Cranston B H, Wheeler J A, Jameson R G and Jacobs J D 2015 Complex changes in plant communities across a subarctic Alpine tree line in Labrador, Canada supplementary appendix table (See Article Tools) *Arctic* **500**
- [45] Harsch M A and Bader M Y 2011 Treeline form—a potential key to understanding treeline dynamics *Glob. Ecol. Biogeogr.* **582**–96
- [46] Danby R K and Hik D S 2007 Variability, contingency and rapid change in recent subarctic alpine tree line dynamics *J. Ecol.* **95** 352–63
- [47] D’Odorico P, He Y, Collins S, De Wekker S F J, Engel V and Fuentes J D 2013 Vegetation-microclimate feedbacks in woodland-grassland ecotones *Glob. Ecol. Biogeogr.* **22** 364–79
- [48] Shugart H H, Saatchi S and Hall F G 2010 Importance of structure and its measurement in quantifying function of forest ecosystems *J. Geophys. Res.* **69**
- [49] Lloyd A H 2005 Ecological histories from Alaskan tree lines provide insight into future change *Ecology* **86** 1687–95
- [50] Ohse B, Jansen F and Wilmking M 2012 Do limiting factors at Alaskan treelines shift with climatic regimes? *Environ. Res. Lett.* **7** 015505
- [51] Henry G H R, Harper K A, Chen W, Deslippe J R, Grant R F, Lafleur P M, Lévesque E, Siciliano S D and Simard S W 2012 Effects of observed and experimental climate change on terrestrial ecosystems in northern Canada: results from the Canadian IPY program *Clim. Change* **115** 207–34
- [52] Gamache I and Payette S 2004 Height growth response of tree line black spruce to recent climate warming across the forest-tundra of eastern Canada *J. Ecol.* **92** 835–45
- [53] Gamache I and Payette S 2005 Latitudinal response of subarctic tree lines to recent climate change in eastern Canada *J. Biogeogr.* **32** 849–62
- [54] Kambo D and Danby R K 2018 Constraints on treeline advance in a warming climate: a test of the reproduction limitation hypothesis *J. Plant Ecol.* **11** 411–22
- [55] Kruse S, Gerdes A, Kath N J, Epp L S, Stoof-Leichsenring K R and Pestryakova L A 2019 Dispersal distances and migration rates at the arctic treeline in Siberia—a genetic and simulation-based study *Biogeosciences* **16** 1211–24
- [56] Hofgaard A and Wilmann B 2002 Plant distribution pattern across the forest-tundra ecotone: the importance of treeline position *Écoscience* **9** 375–85
- [57] Kirilyanov A V, Hagedorn F, Knorre A A, Fedotova E V, Vaganov E A and Naurzbaev M M 2012 20th century tree-line advance and vegetation changes along an altitudinal transect in the Putorana Mountains, northern Siberia *Boreas* **41** 56–67
- [58] Kullman L 2015 Recent and past trees and climates at the arctic/alpine margin in Swedish lapland: an abisko case study review *J. Biodivers. Manage. Forestry* **4**
- [59] Kharuk V I, Im S T, Dvinskaya M L, Ranson K J and Petrov I A 2017 Tree wave migration across an elevation gradient in the Altai mountains, Siberia *J. Mt. Sci.* **14** 442–52
- [60] Bader M Y, Rietkerk M and Bregt A K 2008 A simple spatial model exploring positive feedbacks at tropical alpine treelines *Arct. Antarct. Alp. Res.* **269**–78
- [61] Lloyd A H, Scott Rupp T, Fastie C L and Starfield A M 2002 Patterns and dynamics of treeline advance on the Seward Peninsula, Alaska *J. Geophys. Res.* **107**
- [62] Holtmeier F-K and Broll G 2005 Sensitivity and response of northern hemisphere altitudinal and polar treelines to environmental change at landscape and local scales *Glob. Ecol. Biogeogr.* **14** 395–410
- [63] Cairns D M and Moen J 2004 Herbivory influences tree lines *J. Ecol.* **92** 1019–24
- [64] Körner C 1998 A re-assessment of high elevation treeline positions and their explanation *Oecologia* **115** 445–59
- [65] Hufkens K, Scheunders P and Ceulemans R 2009 Validation of the sigmoid wave curve fitting algorithm on a forest-tundra ecotone in the Northwest Territories, Canada *Ecol. Inform.* **4** 1–7
- [66] Ranson K J, Montesano P M and Nelson R 2011 Object-based mapping of the circumpolar taiga-tundra ecotone with MODIS tree cover *Remote Sens. Environ.* **115** 3670–80
- [67] Ranson K J, Sun G, Kharuk V I and Kovacs K 2004 Assessing tundra-taiga boundary with multi-sensor satellite data *Remote Sens. Environ.* **93** 283–95
- [68] Walther C, Hüttich C, Urban M and Schmulius C 2019 Modelling the Arctic taiga-tundra ecotone using ALOS PALSAR and optical earth observation data *Int. J. Appl. Earth Obs. Geoinf.* **81** 195–206
- [69] Guo W and Rees W G 2019 Altitudinal forest-tundra ecotone categorization using texture-based classification *Remote Sens. Environ.* **232** 111312
- [70] Timoney K P and Mamet S 2020 No treeline advance over the last 50 years in subarctic western and central Canada and the problem of vegetation misclassification in remotely sensed data *Écoscience* **27** 93–106
- [71] Rees G, Brown I, Mikkola K, Virtanen T and Werkman B 2002 How can the dynamics of the tundra-taiga boundary be remotely monitored? *Ambio Spec No* 12 56–62
- [72] Timoney K P, Roi G H and Dale M R T 1993 Subarctic forest-tundra vegetation gradients: the sigmoid wave hypothesis *J. Veg. Sci.* **4** 387–94
- [73] Hofgaard A, Harper K A and Golubeva E 2012 The role of the circumpolar forest-tundra ecotone for Arctic biodiversity *Biodiversity* **13** 174–81
- [74] Walker D A, Reynolds M K, Daniëls F J A, Einarsson E, Elvebakk A and Gould W A 2005 The circumpolar arctic vegetation map *J. Veg. Sci.* **16** 267
- [75] Reynolds M K, Walker D A, Balsler A, Bay C, Campbell M and Cherosov M M 2019 A raster version of the Circumpolar Arctic Vegetation Map (CAVM) *Remote Sens. Environ.* **232** 111297
- [76] Fick S E and Hijmans R J 2017 WorldClim 2: new 1-km spatial resolution climate surfaces for global land areas *Int. J. Climatol.* **37** 4302–15
- [77] Olson D M, Dinerstein E, Wikramanayake E D, Burgess N D, Powell G V N and Underwood E C 2001 Terrestrial ecoregions of the world: a new map of life on earth *BioScience* **51** 933

- [78] Feng M, Sexton J O, Channan S and Townshend J R 2016 A global, high-resolution (30-m) inland water body dataset for 2000: first results of a topographic—spectral classification algorithm *Int. J. Digit. Earth* **9** 113–33
- [79] Hansen M C et al 2013 High-resolution global maps of 21st-century forest cover change *Science* **342** 850–3
- [80] Pekel J-F, Cottam A, Gorelick N and Belward A S 2016 High-resolution mapping of global surface water and its long-term changes *Nature* **540** 418–22
- [81] Feng M, Sexton J O, Huang C, Anand A, Channan S and Song X-P 2016 Earth science data records of global forest cover and change: assessment of accuracy in 1990, 2000, and 2005 epochs *Remote Sens. Environ.* **184** 73–85
- [82] Lehner B and Grill G 2013 Global river hydrography and network routing: baseline data and new approaches to study the world's large river systems *Hydrol. Process.* **27** 2171–86
- [83] Kharuk V I, Ranson K J, Im S T and Naurzbaev M M 2006 Forest-tundra larch forests and climatic trends *Russ. J. Ecol.* **37** 291–8
- [84] Fofonova V, Zhilyaev I, Krayneva M, Yakshina D, Tananaev N and Volkova N 2016 The water temperature characteristics of the Lena River at basin outlet in the summer period *Hydrol. Earth Syst. Sci. Discuss.* **1**–32
- [85] Bolshiyakov D, Makarov A and Savelieva L 2014 Lena River Delta formation during the Holocene *Biogeosciences Discuss.* **12** 4085–122
- [86] Isaev A P, Mikhalyova L G, Solomonov N G, Okoneshnikova M V, Vasilyeva V K and Popov A A 2012 42. Age-old changes in ecosystems of Tit–Ary, the polar island in the lower reaches of the Lena river (north-east Asia) *Cryobiology* **65** 352–3
- [87] Frost G V and Epstein H E 2014 Tall shrub and tree expansion in Siberian tundra ecotones since the 1960s *Glob. Chang. Biol.* **20** 1264–77
- [88] Devi N, Hagedorn F, Moiseev P, Bugmann H, Shiyatov S and Mazepa V 2008 Expanding forests and changing growth forms of Siberian larch at the Polar Urals treeline during the 20th century *Glob. Chang. Biol.* **14** 1581–91
- [89] Kukarskih V V, Devi N M, Moiseev P A, Grigoriev A A and Bubnov M O 2018 Latitudinal and temporal shifts in the radial growth–climate response of Siberian larch in the Polar Urals *J. Mt. Sci.* **15** 722–9
- [90] Shiyatov S G and Mazepa V S 2015 Contemporary expansion of Siberian larch into the mountain tundra of the Polar Urals *Russ. J. Ecol.* **46** 495–502
- [91] Bryn A and Potthoff K 2018 Elevational treeline and forest line dynamics in Norwegian mountain areas – a review *Landsc. Ecol.* **33** 1225–45
- [92] Epstein H E, Myers-Smith I and Walker D A 2013 Recent dynamics of arctic and sub-arctic vegetation *Environ. Res. Lett.* **8** 015040
- [93] Myers-Smith I H, Kerby J T, Phoenix G K, Bjerke J W, Epstein H E and Assmann J J 2020 Complexity revealed in the greening of the arctic *Nat. Clim. Change* **10** 106–17
- [94] Montesano P M, Sun G, Dubayah R O and Jon Ranson K 2016 Spaceborne potential for examining taiga–tundra ecotone form and vulnerability *Biogeosciences* **13** 3847–61
- [95] Kruse S, Gerdes A, Kath N J and Herzschuh U 2018 Implementing spatially explicit wind-driven seed and pollen dispersal in the individual-based larch simulation model: LAVESI-WIND 1.0. *Geosci. Model Dev.* **11** 4451–67
- [96] Dalen L and Hofgaard A 2005 Differential regional treeline dynamics in the scandes mountains *Arct. Antarct. Alp. Res.* **37** 284–96
- [97] Kambo D and Danby R K 2018 Factors influencing the establishment and growth of tree seedlings at Subarctic alpine treelines *Ecosphere* **9** e02176
- [98] Macander M J, Palm E C, Frost G V, Herriges J D, Nelson P R and Roland C 2020 Lichen cover mapping for caribou ranges in interior Alaska and Yukon *Environ. Res. Lett.* **055001**
- [99] Bi J, Xu L, Samanta A, Zhu Z and Myneni R 2013 Divergent arctic-boreal vegetation changes between North America and Eurasia over the past 30 years *Remote Sens.* **5** 2093–112
- [100] Gao M, Piao S, Chen A, Yang H, Liu Q and Fu Y H 2019 Divergent changes in the elevational gradient of vegetation activities over the last 30 years *Nat. Commun.* **10**
- [101] Brazhnik K and Shugart H H 2016 SIBBORK: a new spatially-explicit gap model for boreal forest *Ecol. Modell.* **182**–96
- [102] Foster A C, Armstrong A H, Shuman J K, Shugart H H, Rogers B M and Mack M C 2019 Importance of tree- and species-level interactions with wildfire, climate, and soils in interior Alaska: implications for forest change under a warming climate *Ecol. Modell.* **409** 108765
- [103] Kruse S, Wiczorek M, Jeltsch F and Herzschuh U 2016 Treeline dynamics in Siberia under changing climates as inferred from an individual-based model for *Larix* *Ecol. Modell.* **338** 101–21
- [104] Armstrong A H, Huth A, Osmanoglu B, Sun G, Ranson K J and Fischer R 2020 A multi-scaled analysis of forest structure using individual-based modeling in a costa rican rainforest *Ecol. Modell.* **433** 109226
- [105] Nitze I and Grosse G 2016 Detection of landscape dynamics in the Arctic Lena Delta with temporally dense Landsat time-series stacks *Remote Sens. Environ.* **181** 27–41
- [106] Sulla-Menashe D, Woodcock C E and Friedl M A 2018 Canadian boreal forest greening and browning trends: an analysis of biogeographic patterns and the relative roles of disturbance versus climate drivers *Environ. Res. Lett.* **13** 014007
- [107] Baltzer J L, Veness T, Chasmer L E, Sniderhan A E and Quinton W L 2014 Forests on thawing permafrost: fragmentation, edge effects, and net forest loss *Glob. Chang. Biol.* **20** 824–34
- [108] Thackeray C W, Fletcher C G and Derksen C 2014 The influence of canopy snow parameterizations on snow albedo feedback in boreal forest regions *J. Geophys. Res.* **119** 9810–21
- [109] Saleem A, Bell M A, Kimpe L E, Korosi J B, Arnason J T and Blais J M 2019 Identifying novel treeline biomarkers in lake sediments using an untargeted screening approach *Sci. Total Environ.* **694** 133684
- [110] Harper K A, Danby R K, De Fields D L, Lewis K P, Trant A J and Starzomski B M 2011 Tree spatial pattern within the forest–tundra ecotone: a comparison of sites across Canada *Can. J. Forest Res.* **41** 479–89
- [111] Roy-Léveillé P, Burn C R and McDonald I D 2014 Vegetation-permafrost relations within the forest-tundra ecotone near Old Crow, northern Yukon, Canada *Permafrost Periglac. Process.* **25** 127–35
- [112] Sveinbjörnsson B, Hofgaard A and Lloyd A 2002 Natural causes of the tundra–taiga boundary *Ambio Spec No* **12** 23–29
- [113] Gorelick N, Hancher M, Dixon M, Ilyushchenko S, Thau D and Moore R 2017 Google earth engine: planetary-scale geospatial analysis for everyone *Remote Sens. Environ.* **202** 18–27